

Band-gap change of carbon nanotubes: Effect of small uniaxial and torsional strain

Liu Yang

Thermosciences Institute, NASA Ames Research Center, Mail Stop 230-3, Moffett Field, California 94035-1000

M. P. Anantram,* Jie Han, and J. P. Lu†

NASA Ames Research Center, Mail Stop T27A-1, Moffett Field, California 94035-1000

(Received 15 December 1998; revised manuscript received 11 August 1999)

We use a simple picture based on the π electron approximation to study the band-gap variation of carbon nanotubes with uniaxial and torsional strain. We find (i) that the magnitude of slope of band gap versus strain has an almost universal behavior that depends on the chiral angle, (ii) that the sign of slope depends on the value of $(n-m) \bmod 3$, and (iii) a novel change in sign of the slope of band gap versus uniaxial strain arising from a change in the value of the quantum number corresponding to the minimum band gap. Four orbital calculations are also presented to show that the π orbital results are valid. [S0163-1829(99)00844-9]

I. INTRODUCTION

The mechanical and electronic properties of carbon nanotubes (CNT) have individually been studied in some detail¹⁻⁵ and the predicted dependence of band gap on chirality¹⁻³ has been observed.⁶ The study of band-gap variation with mechanical deformation is important in view of the ability to manipulate individual nanotubes.⁷ Additionally, they could form the basis for nanoscale sensors in a manner similar to experiments using C_{60} molecules.⁸ Recent studies of band-gap change of zig-zag and armchair tubes on mechanical strain have shown interesting behavior.⁹⁻¹¹ References 9 and 10 studied the effect of uniaxial strain using a Green's function method based on the π electron approximation and a four orbital numerical method, respectively. Reference 11 predicted the opening of a band gap in armchair tubes under torsion, using a method that wraps a massless two-dimensional Dirac Hamiltonian on a curved surface. In this paper, we present a simple and unified picture of the band-gap variation of chiral and achiral CNT with uniaxial and torsional strain. The method used is discussed in Sec. II. The results obtained by using a single π orbital are discussed in Sec. III A and are compared to four orbital calculations in Sec. III B. The conclusions are presented in Sec. IV.

II. METHOD

In the presence of a uniform uniaxial and torsional strain, a distorted graphene sheet continues to have two atoms per unit cell (Fig. 1). It is convenient to represent the change in bond lengths using the chirality dependent coordinate system. The axes of the chirality dependent coordinate system corresponding to (n,m) CNT are the line joining the $(0,0)$ and (n,m) carbon atoms (\hat{c}), and its perpendicular (\hat{t}) (Fig. 1).¹² The fixed and chirality dependent coordinate system are related by, $\hat{c} = \cos \theta \hat{x} + \sin \theta \hat{y}$ and $\hat{t} = -\sin \theta \hat{x} + \cos \theta \hat{y}$, where $\sin(\theta) = \frac{1}{2}(n-m/c_h)$ and $\cos(\theta) = \frac{\sqrt{3}}{2}(n+m/c_h)$. $c_h = \sqrt{n^2 + m^2 + nm}$, is the circumference of the tube in units of the equilibrium lattice vector length, $|\vec{a}_1| = |\vec{a}_2| = a_0$. The bond vectors are given by

$$\vec{r}_1 = \frac{a_0}{2} \frac{n+m}{c_h} \hat{c} - \frac{a_0}{2\sqrt{3}} \frac{n-m}{c_h} \hat{t} + \delta \vec{r}_1$$

and (1)

$$\vec{r}_2 = -\frac{a_0}{2} \frac{m}{c_h} \hat{c} + \frac{a_0}{2\sqrt{3}} \frac{2n+m}{c_h} \hat{t} + \delta \vec{r}_2,$$

where $\delta \vec{r}_i$ represents deviation from an undistorted sheet and $\vec{r}_3 = -(\vec{r}_1 + \vec{r}_2)$. Within the context of continuum mechanics, application of a uniaxial or torsional strain causes the following change in the bond vectors of Fig. 1:

$$r_{it} \rightarrow (1 + \epsilon_t) r_{it} \quad \text{and} \quad r_{ic} \rightarrow (1 + \epsilon_c) r_{ic} \quad (\text{tensile}) \quad (2)$$

$$r_{ic} \rightarrow r_{ic} + \tan(\gamma) r_{it} \quad (\text{torsion}), \quad (3)$$

where $i = 1, 2, 3$ and r_{ip} is the p component of \vec{r}_i ($p = c, t$). ϵ_t and ϵ_c represent the strain along \hat{t} and \hat{c} , respectively, in the case of uniaxial strain. γ is the shear strain.

Using Eqs. (1)–(3), the lattice vectors of the distorted sheet are

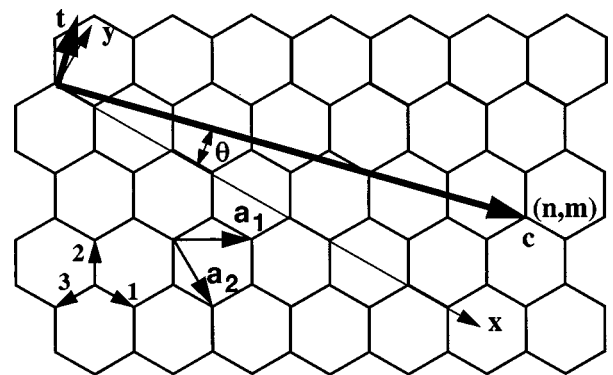


FIG. 1. The fixed (x, y) and chirality dependent (\hat{c}, \hat{t}) coordinates. r_1 , r_2 , and r_3 correspond to bonds 1, 2, and 3, respectively. \vec{a}_1 and \vec{a}_2 are the lattice vectors of the two dimensional sheet.

$$\vec{a}_1 = \vec{r}_1 - \vec{r}_3 = a_0 \left[(1 + \epsilon_c) \frac{1}{2} \frac{2n+m}{c_h} + \tan(\gamma) \frac{\sqrt{3}}{2} \frac{m}{c_h} \right] \hat{c} + a_0 (1 + \epsilon_t) \frac{\sqrt{3}}{2} \frac{m}{c_h} \hat{t} \quad (4)$$

and

$$\vec{a}_2 = \vec{r}_1 - \vec{r}_2 = a_0 \left[(1 + \epsilon_c) \frac{1}{2} \frac{n+2m}{c_h} - \tan(\gamma) \frac{\sqrt{3}}{2} \frac{n}{c_h} \right] \hat{c} - a_0 (1 + \epsilon_t) \frac{\sqrt{3}}{2} \frac{n}{c_h} \hat{t}. \quad (5)$$

The corresponding unit cell area is $|\vec{a}_1 \times \vec{a}_2| = \sqrt{3}/2(1 + \epsilon_t)(1 + \epsilon_c)a_0^2$. The real-space unit cells correspond to $\vec{r} = j_1 \vec{a}_1 + j_2 \vec{a}_2$, where j_1 and j_2 are integers. The one-dimensional (1D) unit cell length (T) is the shortest r_i for which $r_c = 0$. That is, the two lattice points, $\vec{r} = 0$ and $\vec{r} = j_1 \vec{a}_1 + j_2 \vec{a}_2$ have the same \hat{c} coordinate. This corresponds to the following condition on j_i and j_2 ,

$$(1 + \epsilon_c)[j_1(2n+m) + j_2(n+2m)] + \tan(\gamma)\sqrt{3}[j_1m - j_2n] = 0 \quad (6)$$

and the 1D unit cell length is

$$T = a_0(1 + \epsilon_t) \frac{\sqrt{3}}{2} \frac{(j_1m - j_2n)}{c_h}. \quad (7)$$

When only uniaxial strain is present ($\gamma = 0$), Eq. (6) corresponds to, $j_1(2n+m) + j_2(n+2m) = 0$. The corresponding j_1 and j_2 with smallest absolute values are $j_1 = (n+2m)/\text{gcd}(2n+m, n+2m)$ and $j_2 = -(2n+m)/\text{gcd}(2n+m, n+2m)$. gcd refers to the greatest common divisor. Using these values in Eq. (7), the 1D unit cell length of an (n, m) tube is

$$T = (1 + \epsilon_t) \sqrt{3} c_h a_0 / \text{gcd}(2n+m, n+2m). \quad (8)$$

In the absence of strain, Eq. (8) reduces to the result for undeformed nanotubes.⁴ In the presence of uniaxial strain, the unit cell length is equal to $(1 + \epsilon_t)$ times the unstrained unit cell length. When only torsion is present, Eq. (6) simplifies to

$$j_1(2n+m) + j_2(n+2m) + \tan(\gamma)\sqrt{3}(j_1m - j_2n) = 0. \quad (9)$$

For arbitrary values of γ , n , and m , this equation corresponds to a large T . For example, from Fig. 1 it is easy to see that under torsion, the unit cell of an armchair tube can be much larger than a_0 depending on the value of γ . We will come back to this point at the end of Sec. II, where we discuss calculation of band-gap change due to torsion.

We treat the nanotube within the approximation that it is a rolled up graphene sheet and assume a single- π orbital per carbon atom. We calculate the band structure of the distorted sheet to be,¹³

$$E(\vec{k}) = (t_1^2 + t_2^2 + t_3^2 + 2t_1t_2 \cos[\vec{k} \cdot (\vec{r}_1 - \vec{r}_2)] + 2t_2t_3 \cos[\vec{k} \cdot (\vec{r}_2 - \vec{r}_3)] + 2t_3t_1 \cos[\vec{k} \cdot (\vec{r}_3 - \vec{r}_1)])^{1/2}, \quad (10)$$

where $\vec{k} = k_c \hat{c} + k_t \hat{t}$. The primary effects of change in bond vectors are to alter the hopping parameter between carbon atoms and the lattice vectors. The hopping parameter is assumed to scale with bond length as¹⁴ $t_i = t_0(r_0/r_i)^2$, where t_0 and r_0 are the hopping parameter and bond length of an unstrained graphene sheet. The value of t_0 is around 3 eV. From Eqs. (4) and (5), the circumference of the distorted sheet is $(1 + \epsilon_c)c_h a_0$. The wave function of the CNT is quantized around the circumference and so k_c is given by

$$k_c(1 + \epsilon_c)c_h a_0 = 2\pi q, \quad (11)$$

where q is an integer. Equation (10) can now be written as,

$$E(k_t) = \left\{ t_1^2 + t_2^2 + t_3^2 + 2t_1t_2 \cos \left[\pi q \frac{n+2m}{c_h^2} - \frac{\sqrt{3}}{2} \frac{n}{c_h} k'_t a_0 - q \frac{\sqrt{3} \tan(\gamma)}{1 + \epsilon_c} \frac{n}{c_h^2} \right] + 2t_1t_3 \cos \left[\pi q \frac{2n+m}{c_h^2} + \frac{\sqrt{3}}{2} \frac{m}{c_h} k'_t a_0 + \pi q \frac{\sqrt{3} \tan(\gamma)}{1 + \epsilon_c} \frac{m}{c_h^2} \right] + 2t_2t_3 \cos \left[\pi q \frac{n-m}{c_h^2} + \frac{\sqrt{3}}{2} \frac{n+m}{c_h} k'_t a_0 + \pi q \frac{\sqrt{3} \tan(\gamma)}{1 + \epsilon_c} \frac{n+m}{c_h^2} \right] \right\}^{1/2}, \quad (12)$$

where, $k'_t = (1 + \epsilon_t)k_t$. The band gap of an (n, m) tube in presence of uniaxial ($\gamma = 0$) or torsional strain ($\epsilon_c = \epsilon_t = 0$) can be easily calculated from Eq. (12). In case of uniaxial strain, the limits of k_t are given by $-\pi/T < k_t < \pi/T$, where T is the 1D lattice vector length determined by Eq. (8). The number of atoms in the 1D unit cell does not change in the presence of uniaxial strain and so the range of q does not

change from the undeformed case ($q = 0, 1, 2, \dots, N_c$, where N_c is the number of hexagons in the 1D unit cell).

In the case of torsion, the number of atoms in the 1D unit cell and T can be large [Eq. (9)]. The corresponding span of k_t is then small compared to the undeformed tube and the range of q is commensurate with the number of atoms in the 1D unit cell. The eigenspectrum can however be obtained

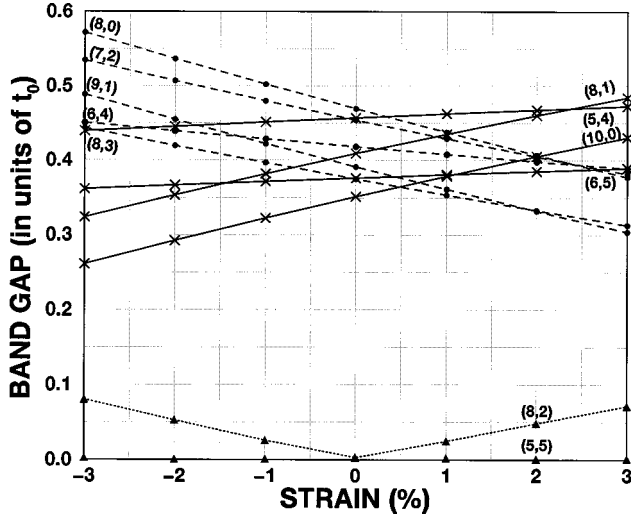


FIG. 2. Band gap versus tensile strain: For semiconducting tubes, the sign of slope of $d(\text{Band gap})/d(\text{Strain})$ depends only on the value of $(n-m) \bmod 3$. The magnitude of $d(\text{Band gap})/d(\text{Strain})$ is largest for zig-zag tubes and decreases with decrease in chiral angle. The magnitude is smallest for armchair tubes. The solid, dashed and dotted lines correspond to $(n-m) \bmod 3$ values of 1, -1 , and 0 respectively. The value of t_0 is around 3 eV.

from Eq. (12) by setting $\gamma=0$ and spanning over the same values of q and k_t as in the undeformed case. This is because the eigen spectrum depends only on the tight-binding parameters (and not on the exact geometry) if the coordination number of the carbon atoms remains constant.¹⁵

III. RESULTS AND DISCUSSION

The results obtained using the method described in Sec. II are discussed in Sec. III A. We then present the results from four orbital calculations with energy minimized structures in Sec. III B.

A. π orbital

We first consider the case of uniaxial strain. The band gap is obtained by finding the minimum of $E(k_t)$, where the span of k_t and q are discussed below Eq. (12). The band-gap change is largest for zig-zag tubes and the magnitude of $|dE_g/d\sigma|$ is approximately equal to $3t_0$. For armchair tubes, application of uniaxial strain does not cause a band gap. We find that, (i) $|dE_g/d\sigma|$ increases with increase in chiral angle (Fig. 2) and (ii) the sign of $dE_g/d\sigma$ follows the $(n-m) \bmod 3$ rule.¹⁶ For example, the chiral angle of (6,5) and (6,4) tubes are close to that of armchair tubes. The slope of band gap versus strain is correspondingly small and the sign of slope are opposite. For semiconducting zig-zag tubes and armchair tubes, our results agree with Ref. 9.

As uniaxial strain increases, there is an abrupt reversal in sign of $dE_g/d\sigma$ as illustrated for zigzag tubes in Fig. 4. This feature indicates a change in band index q corresponding to the band gap and can be understood from the following expression that describes dependence of energy for various values of q at $k_t=0$ [Eq. (A3) of the Appendix]:

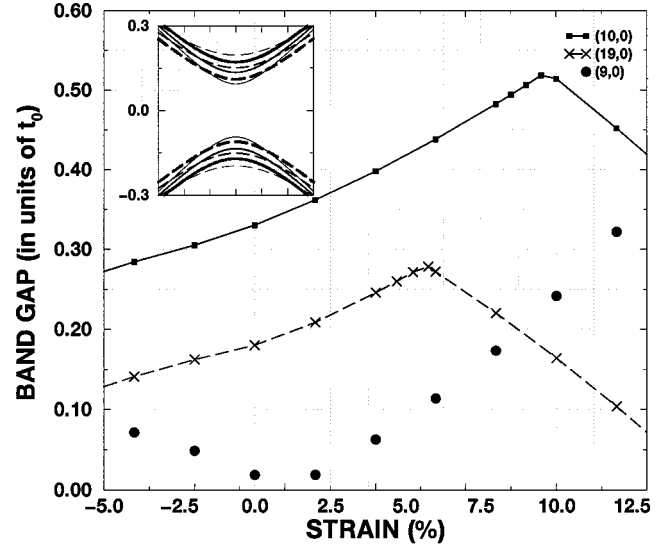


FIG. 3. The change in slope of the (10,0) and (19,0) tubes around 10% and 5% strain, respectively, is due to a change in the quantum number q that yields the minimum band gap. Inset: E vs k of the $q=7$ (solid) and $q=6$ (dashed) bands as a function of strain for a (19,0) tube. Strains of 0%, 3%, and 6% correspond to increasing thickness of the lines.

$$E(0) = E_0(q) - 2t_0 \frac{\delta r_1}{r_0} \left[1 - \frac{2\delta r_2}{\delta r_1} \cos\left(\frac{q\pi}{n}\right) \right] \text{sgn}(q), \quad (13)$$

where $\text{sgn}(q) = [1 - 2\cos(q\pi/n)]$. The minimum value of $E_0(q) = t_0 |1 - 2\cos(q\pi/n)|$ is half of the band gap of an unstrained tube. The first term of Eq. (13) takes the smallest value for the band index $q = q_0$ that satisfies $n = 3q_0 \pm 1$. The second term can however change sign when q changes from q_0 to $q_0 \pm 1$. As a result, a dramatic change in sign of $dE_g/d\sigma$ becomes possible if the magnitude of the second term is larger than change in the first term (Fig. 3). The strain required to observe this effect decreases as the inverse radius for large n . This is because the difference in energy of the q_0 and $q_0 \pm 1$ bands become smaller with increase in radius. Figure 3 demonstrates this point by comparing the (10,0) and (19,0) tubes. For the (19,0) tube, the change in slope occurs at around five percent strain. These strain values are accessible in bulk nanotube samples.¹⁷ The inset of Fig. 3 shows change in energy of the $q=6$ and $q=7$ bands for the (19,0) tube for three different values of strain. While the $q=6$ band shifts up in energy as strain increases, the $q=7$ band shifts down. Thus leading to the discussed change in sign of $dE_g/d\sigma$.

In case of torsional strain, the band gap is obtained by finding the minimum of $E(k_t)$ using Eq. (12), where the span of k_t and q are discussed in the last paragraph of Sec. II. The magnitude of $|dE_g/d\sigma|$ is approximately equal to $3t_0$ for armchair tubes and this is in agreement with Ref. 11. For zig-zag tubes, torsion causes only a small change in band gap. The leading term in band-gap change depends on γ only to second order. We find that (i) $|dE_g/d\sigma|$ decreases with increase in chiral angle and takes the smallest value for zig-zag tubes (Fig. 4) and (ii) the sign of $dE_g/d\sigma$ follows the $(n-m) \bmod 3$ rule.¹⁶

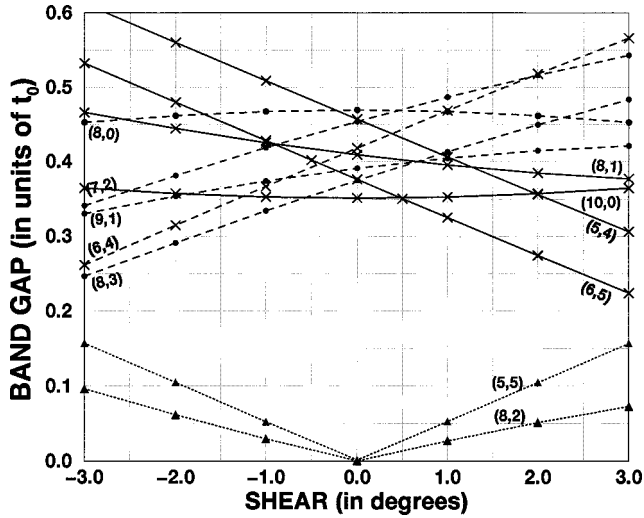


FIG. 4. Band gap versus torsional strain: For semiconducting tubes, the sign of slope of $d(\text{Band gap})/d(\text{Strain})$ depends only on the value of $(n-m) \bmod 3$. The magnitude of $d(\text{Band gap})/d(\text{Strain})$ is largest for armchair tubes and decreases with increase in chiral angle. The magnitude is smallest for zig-zag tubes. The solid, dashed, and dotted lines correspond to $(n-m) \bmod 3$ values of 1, -1 , and 0, respectively.

B. Four orbital

To verify the simple picture presented, we have also performed four orbital calculations using the parametrization given in Ref. 18. The change in bond lengths are computed using both continuum mechanics [Eqs. (2) and (3)] and structures that are energy minimized by Brenner potential.¹⁹ The energy minimization was performed with periodic boundary conditions. For the small values of strain considered, we find that the band gap is not very sensitive to the two methods of obtaining the bond lengths. The results presented in Figs. 5 and 6 correspond to the bond lengths obtained by energy minimization. For semiconducting tubes, the results of Figs. 5 and 6 agree with the π orbital results

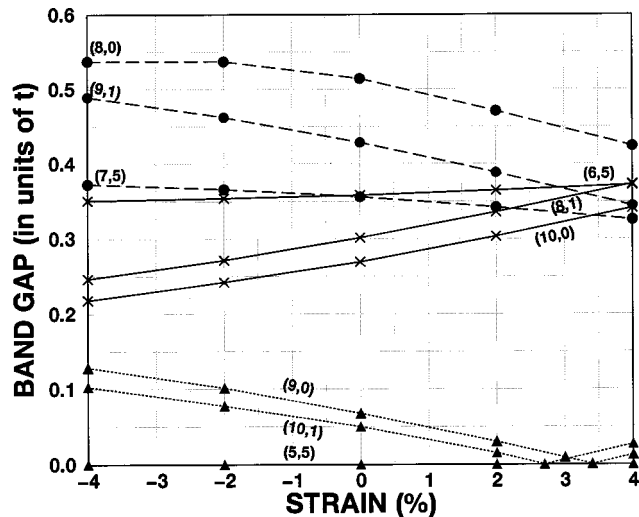


FIG. 5. Same caption as Fig. 2 but these are four orbital results. In the y-axis label, $t = 2.66$ eV.

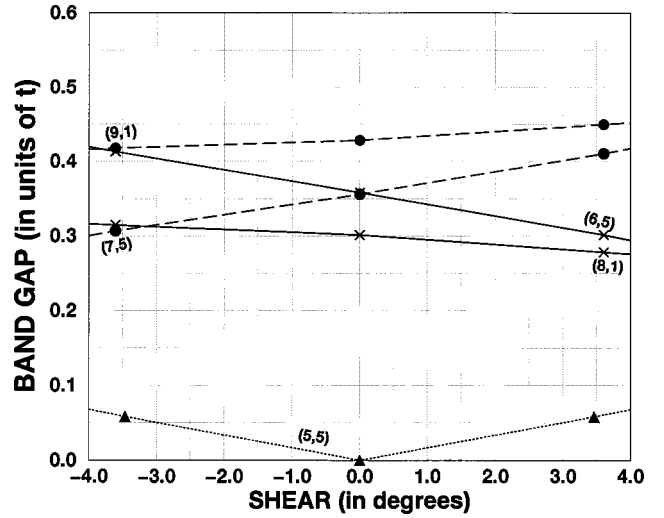


FIG. 6. Same caption as Fig. 4 but these are four orbital results. In the y-axis label, $t = 2.66$ eV.

presented in Figs. 2 and 4, respectively: The slope of $dE_g/d\sigma$ follows the $(n-m) \bmod 3$ rule and the magnitude of slope varies monotonically with chiral angle. The primary difference concerns nonarmchair tubes satisfying $n-m = 3 \times \text{integer}$. This is not surprising because Ref. 2 has predicted such tubes to have a small band gap due to curvature induced hybridization at zero strain. As a result, applying either tension or compression does not produce the “V”-shaped curve of Fig. 2 with zero band gap at zero strain. The difference is that the curves are shifted away from the origin as shown in Fig. 5.

IV. CONCLUSIONS

In conclusion, we present a simple picture to calculate band gap versus strain of CNT with arbitrary chirality. We find that under uniaxial strain, $|dE_g/d\sigma|$ of zig-zag tubes is $3t_0$ independent of diameter, and continually decreases as the chirality changes to armchair, when it takes the value zero. In contrast, we show that under torsional strain, $|dE_g/d\sigma|$ of armchair tubes is $3t_0$ independent of diameter, and continually decreases as the chirality changes to zigzag, where it takes a small value. The sign of $dE_g/d\sigma$ follows the $(n-m) \bmod 3$ rule in both cases.¹⁶ We also predict a change in the sign of $dE_g/d\sigma$ as a function of strain, corresponding to a change in the value of q that corresponds to the band-gap minimum. Comparison to four orbital calculations show that the main conclusions are unchanged. The primary difference involves nonarmchair tubes that satisfy $n-m = 3 \times \text{integer}$.

ACKNOWLEDGMENTS

This work was supported by NASA Contract No. NAS2-14031 to Eloret (L.Y.), NASA Ames Research Center, and the U.S. Department of Energy (J.P.L.).

APPENDIX

Zig-zag tubes under tension: Under uniaxial strain the band structure of $(n,0)$ is [Eq. (12)]

$$E(k_i) = \pm t_2 \left\{ 1 \pm \left(\frac{4t_1}{t_2} \right) \cos\left(\frac{q\pi}{n}\right) \cos\left[(1 + \epsilon_i) \frac{\sqrt{3}}{2} k_i a_0 \right] + \left(\frac{2t_1}{t_2} \right)^2 \cos^2\left(\frac{q\pi}{n}\right) \right\}^{1/2}. \quad (\text{A1})$$

Please note that $t_1 = t_3$ due to symmetry. The minimum of $E(k_i)$ occurs at $k_i = 0$,

$$E(0) = \pm t_2 \left| 1 - \frac{2t_1}{t_2} \cos\left(\frac{q\pi}{n}\right) \right|. \quad (\text{A2})$$

To first order in δr_i Eq. (A2) is²⁰

$$E(0) = E_0(q) - 2t_0 \frac{\delta r_1}{r_0} \left[1 - \frac{2\delta r_2}{\delta r_1} \cos\left(\frac{q\pi}{n}\right) \right] \times \text{sgn}(q) \left[1 - 2 \cos\left(\frac{q\pi}{n}\right) \right], \quad (\text{A3})$$

where, $\text{sgn}(q) = [1 - 2 \cos(q\pi/n)]$ and $E_0(q) = t_0 |1 - 2 \cos(q\pi/n)|$.

*Author to whom correspondence should be addressed. Electronic address: anant@nas.nasa.gov

†Permanent address: CB 3255 Phillips Hall, University of North Carolina–Chapel Hill, Chapel Hill, NC 27599.

¹J. W. Mintmire, B. I. Dunlap, and C. T. White, Phys. Rev. Lett. **68**, 631 (1992).

²N. Hamada, S. Sawada, and A. Oshiyama, Phys. Rev. Lett. **68**, 1579 (1992).

³R. Saito, M. Fujita, G. Dresselhaus, and M. S. Dresselhaus, Appl. Phys. Lett. **60**, 2204 (1992).

⁴M. S. Dresselhaus, G. Dresselhaus, and P. C. Eklund, *Science of Fullerenes and Carbon Nanotubes* (Academic Press, New York, 1996), Chap. 19.

⁵B. I. Yakobson, Appl. Phys. Lett. **72**, 918 (1998); M. B. Nardelli, B. I. Yakobson, and J. Bernholc, Phys. Rev. B **57**, 4277 (1998).

⁶J. W. G. Wildoer, L. C. Venema, A. G. Rinzler, R. E. Smalley, and C. Dekker, Nature (London) **391**, 59 (1998); T. W. Odom, J. L. Huang, P. Kim, and C. M. Lieber, *ibid.* **391**, 62 (1998).

⁷L. C. Venema, J. W. G. Wildoer, H. L. J. T. Tuinstra, C. Dekker, A. G. Rinzler, and R. E. Smalley, Appl. Phys. Lett. **71**, 2629 (1997).

⁸C. Joachim, J. K. Gimzewski, R. R. Schlittler, and C. Chavy, Phys. Rev. Lett. **74**, 2102 (1995).

⁹R. Heyd, A. Charlier, and E. McRae, Phys. Rev. B **55**, 6820 (1997).

¹⁰D. W. Brenner, J. D. Schall, J. P. Mewkill, D. A. Shenderova, and S. B. Sinnott, Interplanet. Soc. **51**, 137 (1998).

¹¹C. L. Kane and E. J. Mele, Phys. Rev. Lett. **78**, 1932 (1997).

¹²C. T. White, D. H. Robertson, and J. W. Mintmire, Phys. Rev. B **47**, 5485 (1993); D. J. Klein, W. A. Seitz, and T. G. Schmalz, J. Phys. Chem. **97**, 1231 (1993); P. J. Lin-Chung and A. K. Rajagopal, J. Phys.: Condens. Matter **6**, 3697 (1994).

¹³This expression can be obtained by extending the treatment of P. R. Wallace, Phys. Rev. **71**, 622 (1947) to the case of a graphene sheet with three bonds with unequal bond lengths and hopping parameters.

¹⁴W. A. Harrison, *Electronic Structure and the Properties of Solids* (Dover, New York, 1989).

¹⁵This discussion applies to the tensile case also, where ϵ_i and ϵ_c should be set equal to zero. At the end of the last paragraph we however did not use this argument to generate the eigenspectrum because the 1D unit cell length simply scales as $(1 + \epsilon_i)$. The essence of this discussion is that if the change in hopping parameters is accounted for, then the eigenspectrum can be calculated by assuming that the geometry has not changed.

¹⁶Defined in terms of $\{-1, 0, 1\}$, i.e., $(n - m) \bmod 3$ equal to 0, 1, and 2 corresponds to 0, 1, and -1 , respectively, in the notation used.

¹⁷D. A. Walters, L. E. Ericson, M. J. Casavant, J. Liu, D. T. Colbert, and R. E. Smalley, Bull. Am. Phys. Soc. **44** (1), 1818 (1999); T. Rueckes, C. L. Cheung, J. W. Hutchinson, and C. M. Lieber, *ibid.* **44** (1), 1818 (1999).

¹⁸D. Tomanek and S. G. Louie, Phys. Rev. B **37**, 8327 (1988).

¹⁹D. W. Brenner, Phys. Rev. B **42**, 9458 (1990).

²⁰ $2t_0 \delta r_i$ can be replaced by δt_i in this expression.